Phase-sensitive near-field imaging of metal nanoparticles

J. Prikulis,[a)] H. Xu, L. Gunnarsson, and M. Käll
Department of Applied Physics, Chalmers University of Technology, SE-412 96 Göteborg, Sweden

H. Olin
Department of Experimental Physics, Chalmers University of Technology, SE-412 96 Göteborg, Sweden

We report on the near-field imaging of silver nanoparticles using an aperture-type near-field microscope operated in illumination mode. The nanoparticles are imaged as interference patterns, due to far-field superposition of the optical fields emitted from the tip and elastically scattered from localized surface plasmons (SP). Aperture-type probe can thus be used to obtain information on the phase shift associated with localized SP coupling at the illumination wavelength. © *2002 American Institute of Physics.* [DOI: 10.1063/1.1516249]

I. INTRODUCTION

Small metal particles possess unique optical properties due to collective electron resonances, so-called localized surface plasmons (SP).[1] When the wavelength of an incident electromagnetic field λ_0 coincides with a SP resonance wavelength λ_{sp}, the scattering cross section of the particle increases tremendously and amplified electric fields are induced near the particle surface. This effect has been heavily exploited in various surface-enhanced spectroscopy experiments.[2,3] An associated phenomenon, that has received considerably less attention, is the phase shift induced by SP coupling, i.e., the phase difference ϕ between the incident field and the field scattered by the excited particle. In a first approximation, one expects that the phase shift should change from $\phi=0$ to $\phi=\pi$ if λ_0 passes λ_{sp} from longer to shorter wavelengths. This effect cannot be observed in ensemble averaged far-field measurements because each particle has different scattering properties and their random spatial position makes interferometric phase measurements impossible.

SP resonance spectra of single gold nanoparticles, measured with aperture-type near-field scanning optical microscopy (NSOM), have been reported by Klar *et al.*[4] The type of information obtained in this measurement was, in principle, similar to a conventional ultraviolet-visible (UV-VIS) spectrum, although the superior spatial resolution allowed for interrogation of single nanoparticles. Similarly, Benrezzak *et al.*, in a scattering-type NSOM (s-NSOM) experiment, investigated how the elastic scattering from gold nanoparticles varies with particle size and illumination wavelength.[5] The near-field spectroscopic properties of Ag particle aggregates have also been studied by Markel *et al.* using a collection mode NSOM.[6] Only recently has the phase of the induced electric fields at the surface of metal particles been studied. Hillenbrand and Keilmann used a s-NSOM, equipped with an interferometric detection system, to simultaneously obtain intensity, phase and topography of individual metal nanoparticles.[7]

In this article we show how the relative phase-shift ϕ can be qualitatively visualized using an aperture NSOM. Single silver nanoparticles or small particle clusters are imaged as circular interference patterns, with the relative intensity of the central peak varying with ϕ. Although the spatial resolution is much worse than what can be obtained in a s-NSOM setup, the advantages are that the present technique can be easily adapted to surface-enhanced spectroscopy measurements of individual nanoparticles or clusters and that the contrast mechanism is relatively simple.

II. EXPERIMENT

We used a commercial NSOM scanner (Nanonics NSOM-100) and Cr–Al coated bent near-field probes with 100 nm apertures obtained from the same manufacturer. Home built electronics and software were used for experiment control and data acquisition. Figure 1 gives a schematic view of the experimental setup. The output from a He–Ne laser (Melles Griot, $\lambda=633$ nm) or an Ar^+ laser (Spectra-Physics, $\lambda=514$, 496, or 488 nm) is coupled into the optical fiber. The NSOM aperture then serves as a subwavelength light source. The distance between the aperture and the surface is controlled by a normal force feedback system.[8] The probe oscillates perpendicularly to the sample surface at the resonance frequency, with a 90%–10% drop in oscillation amplitude within 25 nm of sample movement towards the tip. The set point was kept at 50% of the free oscillation amplitude, which from a simple mechanical model corresponds to an average probe to surface distance of around 25 nm. The elastically scattered light from the nanoparticles, along with the emission from the tip, is collected in the far field by a microscope objective (Nikon 40×, NA=0.4), and detected by an avalanche photodiode (APD). An interference filter blocks the light from the diode laser used for distance regulation. The sample was scanned at a constant speed of 1 μm/s in the lateral direction. The silver sol was prepared using a modified citrate reduction protocol, following Lee and Meisel.[9] The average particle diameter was ≈90 nm, as determined by transmission electron microscopy (TEM) and

---

[a)]Electronic mail: prikulis@fy.chalmers.se
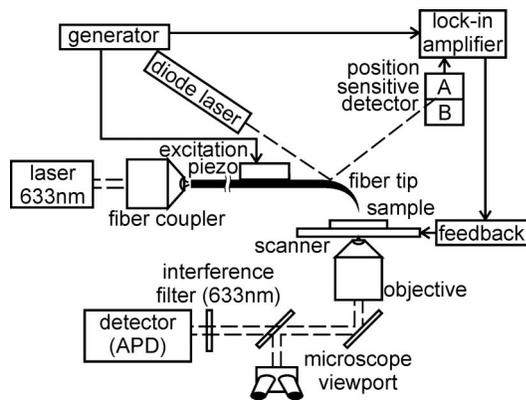
FIG. 1. Schematic view of NSOM setup.

FIG. 3. Measured central optical signal for particles vs their height. The circles, squares and crosses represent measurements from different samples and different NSOM probes. Inset: TEM image of colloidal Ag particles.

UV-VIS spectroscopy. The particles were then immobilized on a polymer coated cover glass according to Freeman *et al.*[10]

III. RESULTS AND DISCUSSION

Figures 2(a) and 2(b) show typical atomic force microscopy (AFM) and NSOM images of colloidal silver particles prepared with the above technique. The detected intensity is

FIG. 2. Simultaneously recorded (a) AFM and (b) NSOM images of colloidal Ag particles. The illumination wavelength was 633 nm. The Z range of the AFM image is around 300 nm. The relative optical signal in the NSOM image varies between $\tilde{I} = -0.6$ (dark) and $\tilde{I} = +0.6$ (bright). Note that positive values of $\tilde{I}$ mean that the far-field output of the NSOM probe is increased by the probe-nanoparticle interaction. (c) Optical profile and NSOM image (inset) of a single Ag particle. (d) Height profile and AFM image (inset) of the same particle.

a result of an interference between the far-field emission from the tapered fiber and the elastically scattered light from the particles on the sample surface. As the sample is scanned in the *x*-*y* plane the recorded NSOM image allows us to compare the particle specific phase shifts induced by the SP coupling to the incident radiation. The absolute intensity is different for different NSOM probes due to variations of the throughput of the taper. We therefore define a dimensionless relative optical signal $\tilde{I} \equiv (I - I_0)/I_0$, where *I* is the measured intensity, and I_0 is the intensity in absence of any particles on the surface. The key observation is that single particles and small aggregates appear as symmetric ring structures with dark ($\tilde{I} < 0$) or bright ($\tilde{I} > 0$) centers in the NSOM images. The distance between successive rings corresponds to approximately $\lambda_0/2$. The NSOM images are not artifact free,[11] however the artifacts are easily identified. The sharp feature on the right from the central maximum in the NSOM image [inset in Fig. 2(c)] is clearly a topographic artifact since it has the same position and shape as the topography in the AFM image of the same particle [inset in Fig. 2(d)]. From the optical profile [Fig. 2(c)] we estimate that the resolution of our NSOM is around 250 nm for this type of experiment. The lateral dimensions of the silver particles are enlarged in the topography image due to tip convolution. We therefore use the height of the particles to characterize their size [Fig. 2(d)]. In Fig. 3 we plot the center intensity versus particle height. Obviously; particles with similar height can have very different central intensity. The reason for this is most probably the irregular shape of the particles, as seen in the TEM image (inset in Fig. 3) and discussed below.

A quantitative analysis of the recorded images would require an elaborate description of the fields emitted from the aperture, including tip-particle coupling effects. Fortunately, the contrast mechanism can be qualitatively understood from a very simple model [Fig. 4(a)]. In a first approximation, light emitted from the tapered fiber can be divided into a propagating wave and an exponentially decaying near field, which causes dipole excitations in particles in the vicinity of the aperture. We approximate the NSOM probe with a point source

$$E_{\text{tip}}(r) \propto \exp[i(kr - \omega t)]\left[\frac{A}{kr} + B\exp(-r/\eta)\right]. \quad (1)$$

The constants *A* and *B* define the amplitudes of the far-field and near-field contributions, respectively, *r* is the distance
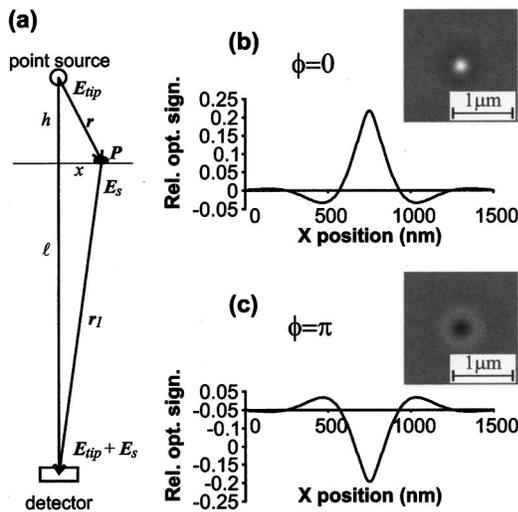
FIG. 4. (a) Model geometry for contrast formation (not in scale). (b,c) Simulation results from the simple dipole model with $\lambda = 633$ nm, distance between the aperture and the sample $h = 25$ nm, $\eta = \lambda/4$, $A = 1$, $B = 100$, $\ell = 3$ cm, $|\alpha| = 1.32 \times 10^{-34}$ Cm^2 V^{-1}, which corresponds to electrostatic dipole polarizability of a Ag sphere with 10 nm radius at $\lambda = 633$ nm, in the two extreme cases $\phi = 0$ and $\phi = \pi$.

FIG. 5. (a) Measured ensemble-averaged extinction spectrum of silver particles deposited on cover glass. (b) Amplitude and phase of the polarizability α calculated in the electrostatic approximation for an Ag sphere and an ellipsoid with aspect ratio 1.5 in a dielectric surrounding medium with refractive index $n = 1.3$.

from the light source, k is the wave number, ω is the angular frequency, and η is the near-field decay length. Choosing the ratio $B/A = 100$, and ignoring the heat dissipation of the incident intensity in the NSOM probe, corresponds to a taper throughput of approximately $T = 10^{-4}$. A dipole moment $P = \alpha E_{\text{tip}}(r)$ is induced in the particle. The oscillating dipole emits scattered waves $E_s(r_1) \approx Z_0 k^2/(4\pi i k r_1) dP/dt \exp(-ikr_1)$ which superimpose with the far-field emission from the fiber at the detector. Here Z_0 is the free space impedance. The measured intensity is thus approximately given by

$$I \propto \int_0^{2\pi/\omega} \mathsf{R}[E_{\text{tip}}(\ell) + E_s(r_1)]^2 dt, \qquad (2)$$

where R denotes the real part and ℓ is the distance between the light source and the detector. The phase of the complex nanoparticle polarizability $\alpha = |\alpha| e^{i\phi}$ determines whether the particle appears with a dark or a bright center in the NSOM image, as shown in Figs. 4(b) and 4(c).

Figure 5(a) demonstrates that the ensemble averaged far-field extinction spectrum of the silver nanoparticles exhibits surface-plasmon peaks over a broad region, approximately centered at the He–Ne measurement wavelength. However, Mie theory calculations for small silver spheres (not shown here) produce SP resonances in the blue-green region. The obvious redshift of the extinction spectrum in this particular case, compared to what is expected for spherical Ag particles, indicates that elongated particles or nanoparticle aggregates, give a dominant contribution to the far-field extinction. The huge variation of the optical signal for particles with similar height (Fig. 3) also indicates that the shape of the particles or clusters determines the phase of the near-field SP coupling at the measurement wavelength. This is also supported by polarizability calculations for ellipsoids in the electrostatic approximation,[12] which shows that a small elon-

gation of the particle causes a significant redshift [Fig. 5(b)]. The same effect has been observed by Gotschy *et al.* in extinction measurements on arrays of nano-fabricated ellipsoids.[13] Small particles with diameter less than 60 nm always appear bright in the NSOM images, because their resonance wavelength is much shorter than the illumination wavelength, as can be seen in Fig. 3. This is also in agreement with observations by Emory, Haskins, and Nie[14] for samples similar to ours, which showed that smaller particles have shorter optimal excitation wavelengths for surface enhanced Raman scattering.

In order to verify the model, we recorded a series of NSOM images of the same area at different wavelengths (Fig. 6). At 633 nm illumination wavelength almost all particles appear with bright centers, surrounded by distinctive
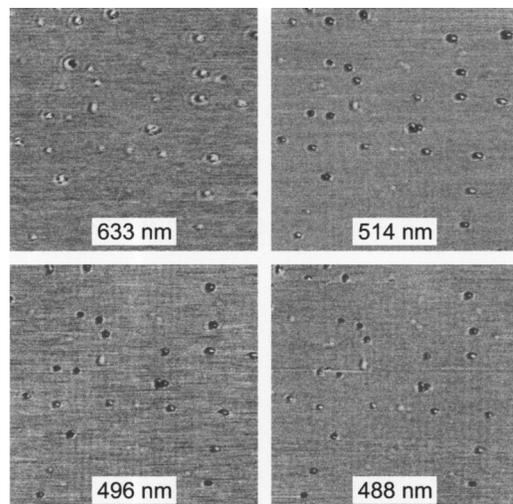
FIG. 6. NSOM images of Ag particles recorded at different wavelengths. The image area is 20 μm $\times$ 20 μm.

interference rings. As expected, when the wavelength is lowered, more and more particles appear with a dark center in the NSOM image.

IV. CONCLUSIONS

In conclusion, we have demonstrated a method for phase-sensitive imaging of metal nanoparticles using aperture NSOM. In comparison to s-NSOM measurements on similar samples[5,7] the spatial resolution is poor. However, aperture NSOM has higher near-field intensity compared to back-ground radiation and is therefore better suited for localized spectroscopy experiments, such as surface enhanced fluorescence or Raman scattering. A simple model of contrast formation gives qualitatively correct results for realistic parameters.

[1] U. Kreibig and M. Vollmer, *Optical Properties of Metal Clusters* (Springer, Berlin, 1995).

[2] K. Kneipp, H. Kneipp, I. Itzkan, R. R. Dasari, and M. S. Feld, Chem. Rev. **99**, 2957 (1999).

[3] M. Moskovits, Rev. Mod. Phys. **57**, 783 (1985).

[4] T. Klar, M. Perner, S. Grosse, G. von Plessen, W. Spirkl, and J. Feldmann, Phys. Rev. Lett. **80**, 4249 (1998).

[5] S. Benrezzak, P. M. Adam, J. L. Bijeon, and P. Royer, Surf. Sci. **491**, 195 (2001).

[6] V. A. Markel, V. A. Shalaev, P. Zhang, W. Huynh, L. Tay, T. I. Haslett, and M. Moskovits, Phys. Rev. B **59**, 10903 (1999).

[7] R. Hillenbrand and F. Keilmann, Appl. Phys. B: Lasers Opt. **73**, 239 (2001).

[8] J. F. Wolf, P. E. Hillner, R. Bilewicz, P. Kölsch, and J. P. Rabe, Rev. Sci. Instrum. **70**, 2751 (1999).

[9] P. C. Lee and D. Meisel, J. Phys. Chem. **86**, 3391 (1982).

[10] R. G. Freeman, K. C. Grabar, K. J. Allison, R. M. Bright, J. A. Davis, A. P. Guthrie, M. B. Hommer, M. A. Jackson, P. C. Smith, D. G. Walter, and M. J. Natan, Science **267**, 1629 (1995).

[11] B. Hecht, H. Bielefeldt, Y. Inouye, D. W. Pohl, and L. Novotny, J. Appl. Phys. **81**, 2492 (1997).

[12] C. F. Bohren and D. R. Huffman, *Absorption and Scattering of Light by Small Particles* (Wiley, New York, 1998).

[13] W. Gotschy, K. Vonmetz, A. Leitner, and F. R. Aussenegg, Opt. Lett. **21**, 1099 (1996).

[14] S. R. Emory, W. E. Haskins, and S. Nie, J. Am. Chem. Soc. **120**, 8009 (1998).